

# Product and Ratio of Two $\alpha - \kappa - \mu$ Shadowed Random Variables and its Application to Wireless Communication

Shashank Shekhar, Sheetal Kalyani

Department of Electrical Engineering,  
Indian Institute of Technology, Madras,  
Chennai, India 600036.

{ee17d022@smail,skalyani@ee}.iitm.ac.in

arXiv:2407.10250v1 [cs.IT] 14 Jul 2024

## Abstract

This work studies the product and ratio statistics of independent and non-identically distributed (i.n.i.d)  $\alpha - \kappa - \mu$  shadowed random variables. We derive the series expression for the probability density function (PDF), cumulative distribution function (CDF), and moment generating function (MGF) of the product and ratio of i.n.i.d  $\alpha - \kappa - \mu$  shadowed random variables. We then give the single integral representation for the derived PDF expressions. Further, as application examples, 1) outage probability has been derived for cascaded wireless systems, and 2) physical-layer security metrics like secrecy outage probability and strictly positive secrecy capacity are derived for the classic three-node model with  $\alpha - \kappa - \mu$  shadowed fading. Next, we discuss an intelligent reflecting surface-assisted communication system over  $\alpha - \kappa - \mu$  shadowed fading.

## Index Terms

$\alpha - \kappa - \mu$  shadowed fading, Product & Ratio statistics, Cascade channel, Mellin transformation

## I. INTRODUCTION

A wireless channel is governed mainly by two physical phenomena: shadowing (which results in long-term signal variation) and multipath (which results in short-term fading). Shadowing is typically modeled using lognormal distribution [1] or sometimes using gamma distribution [2].

In contrast to shadowing, the multipath effect is characterized by a broad range of distributions such as Rayleigh, Rician, Nakagami- $m$ , Hoyt, and more general distributions like  $\kappa - \mu$ ,  $\eta - \mu$  [3]. The  $\kappa - \mu$  shadowed distribution introduced in [4] provides a natural generalization of the  $\kappa - \mu$  fading where the line-of-sight (LOS) component of the received signal is random, *i.e.*, subject to shadowing. This type of fading model is known as the LOS shadow fading model in the literature.

All the fading models mentioned above, including  $\kappa - \mu$  shadowed and its special cases, assume a homogeneous scattering environment where the intensity of the received signal is the sum of the intensity of different multipath components [5]. To generalize these models and characterize the non-linearity of the propagation medium, a new parameter  $\alpha$  was introduced in [5]. Recently, a generalization of  $\kappa - \mu$  shadowed distribution is discussed in [6] that incorporates the non-linearity of the propagation environment. This fading distribution is known as  $\alpha - \kappa - \mu$  shadowed distribution where the parameter  $\alpha \in \mathbb{R}^+$  determines the non-linearity of the propagation environment.

In the literature, Fisher - Snedecor  $\mathcal{F}$  distribution [7] is also suggested for modeling small-scale fading. The properties of Fisher - Snedecor  $\mathcal{F}$  distribution and its related distributions are discussed in [7], [8]. The physical model of Fisher - Snedecor  $\mathcal{F}$  distribution is similar to the Nakagami- $m$  fading model with modification to incorporate the shadowing effect by multiplying an inverse Nakagami- $m$  random variable (RV). However, this fading model results in a simple form for probability density function (PDF) and cumulative distribution function (CDF) expression. This fading model does not include the various generalized fading models such as  $\kappa - \mu$  fading, Rician fading, and others as special cases. Also, the Fisher - Snedecor  $\mathcal{F}$  distribution does not incorporate the non-linearity of the propagation environment, which is modeled in  $\alpha - \kappa - \mu$  shadowed fading by parameter  $\alpha$ .

In a variety of wireless communication applications, such as relay-based communication systems [9], and intelligent reflecting surfaces (IRS) assisted communication system [10]–[12], the transmitted signal from the source reaches the destination after experiencing a couple of fading environments. To analyze such a communication system's performance, one needs to know the statistics of the product of corresponding fading distributions. Hence, the statistical characterization of the product of two RVs is crucial in wireless communication. Similarly, the ratio of random variables appears in scenarios like the study of signal-to-interference ratio and secrecy analysis. A frequency domain based approach is presented in [13] to evaluate the

metrics related to physical layer security in wireless systems. The study of product and ratio of probability distribution has been an area of interest for statisticians for a long time. The product and ratio statistics of  $H$ -distribution were studied in [14]. For example, in bistatic scatter radio communication, the indirect channel between carrier emitter and software-defined radio (SDR) reader through a radio frequency (RF) tag is modeled as the product of two Rayleigh and Rician fading channels in [15] and [16], respectively. A close approximation for the product of independent Rayleigh RVs is proposed in [17]. The work in [15] and [16] were focused on point-to-point communication. In contrast, a multi-scatter scenario is considered in [18] where multiple carrier emitters are present, and each channel is modeled as Nakagami- $m$  fading. Hence, the channel between the carrier emitter and the SDR reader is a product of two Nakagami- $m$  RVs. In [19], authors presented a general result for the product statistics of Rayleigh fading. A generic cascaded channel has been considered in [20], [21] with Nakagami- $m$  and generalized Nakagami- $m$  fading, respectively. An IRS-assisted wireless communication system under Nakagami- $m$  fading was studied in [22]. The authors in [23] considered an IRS-assisted communication system where each link undergoes  $\kappa - \mu$  fading; hence, the link between source to IRS and IRS to destination is the product of two  $\kappa - \mu$  RVs. Authors in [24] studied the product statistics of two independent and non-identically distributed (i.n.i.d.)  $\kappa - \mu$  RVs. In [25] the statistical characterization of the product of two i.n.i.d.  $\alpha - \mu$ ,  $\eta - \mu$  and  $\kappa - \mu$  RVs is done. The author in [26] studied the product statistics of two i.n.i.d.  $\kappa - \mu$  shadowed RVs.

In this work, we are interested in  $\alpha - \kappa - \mu$  shadowed fading since it encompasses various popular fading models such as one-sided Gaussian, Rayleigh, Rician, Nakagami- $m$ ,  $\kappa - \mu$ ,  $\eta - \mu$  [3], Rician shadowed [27] and  $\kappa - \mu$  shadowed [4]. Other than this, the  $\alpha - \kappa - \mu$  shadowed fading has received a lot of traction in the wireless community in recent literature like [28]–[30]. Recently, authors in [31] approximated the  $\alpha - \kappa - \mu$  shadowed RV with generalized Gamma RV and used it to analyze secure ultra-reliable and low latency communications systems. This motivates us to look at the product and ratio statistics of  $\alpha - \kappa - \mu$  shadowed fading. We provided the statistical characterization of the product and ratio of two independent non-identically distributed (i.n.i.d.)  $\alpha - \kappa - \mu$  shadowed RVs. The closed-form exact expressions for PDF and CDF of the considered RVs are derived using Mellin transformation. The contribution and utility of this work are summarized as follows:

- Series expressions for PDF, CDF, and MGF of the product and ratio of two, i.n.i.d.  $\alpha - \kappa - \mu$  shadowed RV are derived using the direct application of Mellin transform.

- We have derived a novel Laplace-type integral representation for the derived PDF expression of the product and ratio statistics.
- We presented the performance metrics for a cascaded wireless system, physical layer security, and outage probability (OP) for an IRS-assisted wireless communication system as application examples for the derived theoretical results to highlight the utility of this work.
- The results derived here generalize many existing results in the literature. For example, the cascade wireless system results presented in [24]–[26] can be easily deduced from our results. Similarly, our results on physical layer security generalize works in [29], [32]–[35]. The OP expressions derived for an IRS-assisted wireless communication system in [36]–[38] are the special cases of our derived expression.

## II. DEFINITIONS AND PROBLEM STATEMENT

In  $\alpha - \kappa - \mu$  shadowed fading environment, the received signal envelope  $R$  is as follows [6]

$$R^\alpha = \sum_{i=1}^{\mu} [(P_i + \xi p_i)^2 + (Q_i + \xi q_i)^2], \quad (1)$$

where  $\alpha \in \mathbb{R}^+$  characterizes the non-linearity of the propagation medium.  $\mu$  denotes the number of multipath clusters. In each cluster, the scattered components  $P_i, Q_i$  are modeled as  $\mathcal{N}(0, \sigma^2)$ . The dominant components are characterized by real numbers  $p_i, q_i$ , and RV  $\xi$  that follows Nakagami- $m$  distribution with shape parameter  $m$  and spread parameter  $\Omega = 1$ . The set of parameters  $\{\alpha, \kappa, \mu, m\}$  completely defines the  $\alpha - \kappa - \mu$  shadowed fading model. The parameter  $\kappa = \sum_{i=1}^{\mu} (p_i^2 + q_i^2) / 2\sigma^2$  signifies the ratio of dominant component power and scattered component power.

We considered two independent non-identically distributed (i.n.i.d)  $\alpha - \kappa - \mu$  shadowed RVs, say  $X_i$  with mean  $\bar{\gamma}_i$  and non-negative real shaping parameters  $\alpha_i, \kappa_i, \mu_i, m_i$  for  $i = 1, 2$ . Each  $X_i$  follows the distribution given by [6, Eq. (4)],

$$f_{X_i}(x_i) = \frac{\theta_i \alpha_i}{2c_i^{\mu_i} \bar{\gamma}_i} \left(\frac{x_i}{\bar{\gamma}_i}\right)^{\frac{\alpha_i \mu_i}{2} - 1} \exp\left(-\frac{1}{c_i} \left(\frac{x_i}{\bar{\gamma}_i}\right)^{\frac{\alpha_i}{2}}\right) \times {}_1F_1\left(m_i; \mu_i; \frac{\beta_i}{c_i} \left(\frac{x_i}{\bar{\gamma}_i}\right)^{\frac{\alpha_i}{2}}\right), \quad (2)$$

where  $i = 1, 2$ ,  $\theta_i = \frac{m_i^{m_i}}{\Gamma(\mu_i)(\mu_i\kappa_i+m_i)^{m_i}}$ ,  $\beta_i = \frac{\mu_i\kappa_i}{(\mu_i\kappa_i+m_i)}$ ,  ${}_1F_1(\cdot; \cdot; \cdot)$  is confluent hypergeometric function [39] and

$$c_i = \left( \frac{1}{\theta_i \Gamma\left(\mu_i + \frac{2}{\alpha_i}\right) {}_2F_1\left(m_i, \mu_i + \frac{2}{\alpha_i}; \mu_i; \beta_i\right)} \right)^{\frac{\alpha_i}{2}}, \quad (3)$$

where,  ${}_2F_1(\cdot, \cdot; \cdot; \cdot)$  is Gauss hypergeometric function [39]. Our objective is to statistically characterize the RV  $Y = X_1 X_2$  and  $Z = \frac{X_1}{X_2}$ . The following sections will provide the analytical expression for PDF, CDF, and MGF of RV  $Y$  and  $Z$ .

### III. STATISTICAL CHARACTERIZATION OF PRODUCT STATISTICS

In this section, We derive the probability density function (PDF), cumulative distribution function (CDF), and moment generating function (MGF) of RV  $Y$ , *i.e.*, the product of two  $\alpha - \kappa - \mu$  shadowed RVs by using the technique of Mellin transform. From the definition of Mellin transform [40, Eq. (2.8.9)] and [6, Eq. (8)], we have

$$\begin{aligned} \mathcal{M}[f_{X_i}(x_i); s] &= \theta_i \bar{\gamma}_i^{s-1} c_i^{\frac{2(s-1)}{\alpha_i}} \Gamma\left(\mu_i + (s-1)\frac{2}{\alpha_i}\right) \\ &\times {}_2F_1\left(m_i, \mu_i + (s-1)\frac{2}{\alpha_i}; \mu_i; \beta_i\right), \end{aligned} \quad (4)$$

It is a well-known fact that the Mellin convolution of individual PDFs gives the PDF of the product of two independent RVs, and the Mellin transform of the said PDF is the product of the Mellin transform of corresponding PDFs [40]. Hence, the Mellin transform of  $Y$  is

$$\begin{aligned} \mathcal{M}[f_Y(y); s] &= \mathcal{M}[f_{X_1}(x_1); s] \mathcal{M}[f_{X_2}(x_2); s] \\ &= \theta_1 \theta_2 (\bar{\gamma}_1 \bar{\gamma}_2)^{s-1} c_1^{\frac{2(s-1)}{\alpha_1}} c_2^{\frac{2(s-1)}{\alpha_2}} \\ &\times \Gamma\left(\mu_1 + (s-1)\frac{2}{\alpha_1}\right) \Gamma\left(\mu_2 + (s-1)\frac{2}{\alpha_2}\right) \\ &\times {}_2F_1\left(m_1, \mu_1 + (s-1)\frac{2}{\alpha_1}; \mu_1; \beta_1\right) \\ &\times {}_2F_1\left(m_2, \mu_2 + (s-1)\frac{2}{\alpha_2}; \mu_2; \beta_2\right). \end{aligned} \quad (5)$$

Note that  $\beta_1, \beta_2 < 1$  and  $\mu_1, \mu_2 > 0$  so both the hypergeometric function present in the Mellin transform of  $Y$  converges  $\forall s$ . Using the series expansion of hypergeometric function [39, Eq. (1.1.18)], we have

$$\begin{aligned} \mathcal{M}[f_Y(y); s] &= \frac{\theta_1 \theta_2 c_1^{-\frac{2}{\alpha_1}} c_2^{-\frac{2}{\alpha_2}}}{\bar{\gamma}_1 \bar{\gamma}_2} \sum_{u,v=0}^{\infty} \frac{(m_1)_u (m_2)_v \beta_1^u \beta_2^v}{(\mu_1)_u (\mu_2)_v u! v!} \\ &\times \Gamma\left(\mu_1 + u - \frac{2}{\alpha_1} + \frac{2}{\alpha_1} s\right) \\ &\times \Gamma\left(\mu_2 + v - \frac{2}{\alpha_2} + \frac{2}{\alpha_2} s\right) \left(\frac{c_1^{-\frac{2}{\alpha_1}} c_2^{-\frac{2}{\alpha_2}}}{\bar{\gamma}_1 \bar{\gamma}_2}\right)^{-s} \end{aligned} \quad (6)$$

Now,  $f_Y(y)$  is obtained using the inverse Mellin transform [41, Eq. 2.8], *i.e.*,

$$f_Y(y) = \delta \theta_1 \theta_2 \sum_{u,v=0}^{\infty} A_{u,v} H_{0,2}^{2,0} \left[ \delta y \left| \begin{matrix} - \\ (b_1, \frac{2}{\alpha_1}), (b_2, \frac{2}{\alpha_2}) \end{matrix} \right. \right], \quad (7)$$

where  $A_{u,v} = \frac{(m_1)_u (m_2)_v \beta_1^u \beta_2^v}{(\mu_1)_u (\mu_2)_v u! v!}$ ,  $\delta = \frac{c_1^{-\frac{2}{\alpha_1}} c_2^{-\frac{2}{\alpha_2}}}{\bar{\gamma}_1 \bar{\gamma}_2}$ ,  $b_1 = \mu_1 + u - \frac{2}{\alpha_1}$ ,  $b_2 = \mu_2 + v - \frac{2}{\alpha_2}$ , and  $H_{p,q}^{m,n} \left[ x \left| \begin{matrix} (a_p, A_p) \\ (b_q, B_q) \end{matrix} \right. \right]$

is the H-function defined in [41, Eq. 1.1]. Equation (7) provides the PDF of the product of two  $\alpha - \kappa - \mu$  shadowed RV in the form of double infinite summation.

### A. Cumulative Distribution Function

The CDF of RV  $Y$ , *i.e.*,  $F_Y(y) = \int_0^y f_Y(t) dt$  follows from the definition of H-function and given as

$$\begin{aligned} F_Y(y) &= \delta \theta_1 \theta_2 \sum_{u,v=0}^{\infty} A_{u,v} \frac{1}{2\pi i} \int_C \Gamma\left(b_1 + \frac{2}{\alpha_1} s\right) \\ &\times \Gamma\left(b_2 + \frac{2}{\alpha_2} s\right) \left(\int_0^y (\delta t)^{-s} dt\right) ds \end{aligned} \quad (8)$$

After solving the inner integral and substituting the limits, we have

$$\begin{aligned} F_Y(y) &= \delta \theta_1 \theta_2 y \sum_{u,v=0}^{\infty} A_{u,v} \\ &\times H_{1,3}^{2,1} \left[ \delta y \left| \begin{matrix} (-1, 1) \\ (b_1, \frac{2}{\alpha_1}), (b_2, \frac{2}{\alpha_2}), (0, 1) \end{matrix} \right. \right], \\ &\stackrel{(a)}{=} \theta_1 \theta_2 \sum_{u,v=0}^{\infty} A_{u,v} H_{1,3}^{2,1} \left[ \delta y \left| \begin{matrix} (0, 1) \\ (b_3, \frac{2}{\alpha_1}), (b_4, \frac{2}{\alpha_2}), (1, 1) \end{matrix} \right. \right], \end{aligned} \quad (9)$$

where  $b_3 = \mu_1 + u$ ,  $b_4 = \mu_2 + v$  and (a) follows from a functional relation given in [41, Property 1.5, Eq. 1.60]. Next, we derive the closed-form/analytical expression for the MGF of RV  $Y$ .

### B. Moment Generating Function

The moment generating function (MGF) of an RV is directly related to the Laplace transform of PDF as

$$M_Y(s) = \mathcal{L}[f_Y(y); -s]. \quad (10)$$

Substituting (9) in (10) and then using the identity [41, Eq. 2.19], we have

$$\begin{aligned} M_Y(s) &= \theta_1 \theta_2 \sum_{u,v=0}^{\infty} A_{u,v} \\ &\times H_{1,2}^{2,1} \left[ \frac{\delta}{(-s)} \left| \begin{matrix} (1, 1) \\ (b_3, \frac{2}{\alpha_1}), (b_4, \frac{2}{\alpha_2}) \end{matrix} \right. \right], \end{aligned} \quad (11)$$

### C. Higher Moments of $Y$

The  $n$ -th order moment of RV  $Y$  is given by  $\mathbb{E}[Y^n] = \mathbb{E}[X_1^n] \mathbb{E}[X_2^n]$ , since  $X_1$  and  $X_2$  are independent RVs. Also, note that the  $\mathbb{E}[Y^n] = \mathcal{M}[f_Y(y); s] |_{s=n+1}$ . Hence, from (5) we have

$$\begin{aligned} \mathbb{E}[Y^n] &= \theta_1 \theta_2 (\bar{\gamma}_1 \bar{\gamma}_2)^n c_1^{\frac{2n}{\alpha_1}} c_2^{\frac{2n}{\alpha_2}} \Gamma\left(\mu_1 + \frac{2n}{\alpha_1}\right) \\ &\times \Gamma\left(\mu_2 + \frac{2n}{\alpha_2}\right) {}_2F_1\left(m_1, \mu_1 + \frac{2n}{\alpha_1}; \mu_1; \beta_1\right) \\ &\times {}_2F_1\left(m_2, \mu_2 + \frac{2n}{\alpha_2}; \mu_2; \beta_2\right). \end{aligned} \quad (12)$$

## IV. STATISTICAL CHARACTERIZATION OF RATIO STATISTICS

In this section, We derive the PDF, CDF, and MGF of RV  $Z$ , *i.e.*, the ratio of two  $\alpha - \kappa - \mu$  shadowed RVs. Note that the Mellin transform of the ratio of two independent RVs is related to their individual Mellin transform as follows

$$\begin{aligned} \mathcal{M}[f_Z(z); s] &= \mathcal{M}[f_{X_1}(x_1); s] \mathcal{M}[f_{X_2}(x_2); 2-s], \\ &= \theta_1 \theta_2 (\bar{\gamma}_1)^{s-1} (\bar{\gamma}_2)^{1-s} c_1^{\frac{2(s-1)}{\alpha_1}} c_2^{\frac{2(1-s)}{\alpha_2}} \\ &\times \Gamma\left(\mu_1 + (s-1) \frac{2}{\alpha_1}\right) \Gamma\left(\mu_2 + (1-s) \frac{2}{\alpha_2}\right) \\ &\times {}_2F_1\left(m_1, \mu_1 + (s-1) \frac{2}{\alpha_1}; \mu_1; \beta_1\right) \\ &\times {}_2F_1\left(m_2, \mu_2 + (1-s) \frac{2}{\alpha_2}; \mu_2; \beta_2\right). \end{aligned} \quad (13)$$

Again using the series expansion of  ${}_2F_1(\cdot, \cdot; \cdot; \cdot)$ , we have

$$\begin{aligned} \mathcal{M}[f_Z(z); s] &= \frac{\theta_1 \theta_2 \bar{\gamma}_2 c_1^{-\frac{2}{\alpha_1}} c_2^{\frac{2}{\alpha_2}}}{\bar{\gamma}_1} \sum_{u,v=0}^{\infty} \frac{(m_1)_u (m_2)_v \beta_1^u \beta_2^v}{(\mu_1)_u (\mu_2)_v u! v!} \\ &\times \Gamma\left(\mu_1 + u - \frac{2}{\alpha_1} + \frac{2}{\alpha_1} s\right) \\ &\times \Gamma\left(\mu_2 + v + \frac{2}{\alpha_2} - \frac{2}{\alpha_2} s\right) \left(\frac{\bar{\gamma}_2 c_1^{-\frac{2}{\alpha_1}} c_2^{\frac{2}{\alpha_2}}}{\bar{\gamma}_1}\right)^{-s} \end{aligned} \quad (14)$$

Now,  $f_Z(z)$  is obtained using the inverse Mellin transform [41, Eq. 2.8], *i.e.*,

$$f_Z(z) = \zeta \theta_1 \theta_2 \sum_{u,v=0}^{\infty} A_{u,v} H_{1,1}^{1,1} \left[ \zeta z \left| \begin{array}{c} \left(a_1, \frac{2}{\alpha_2}\right) \\ \left(b_1, \frac{2}{\alpha_1}\right) \end{array} \right. \right], \quad (15)$$

where  $\zeta = \frac{\bar{\gamma}_2 c_1^{-\frac{2}{\alpha_1}} c_2^{\frac{2}{\alpha_2}}}{\bar{\gamma}_1}$  and  $a_1 = 1 - \mu_2 - v - \frac{2}{\alpha_2}$ . Following the similar steps as in the calculation of  $F_Y(y)$ , we have

$$F_Z(z) = \theta_1 \theta_2 \sum_{u,v=0}^{\infty} A_{u,v} H_{2,2}^{1,2} \left[ \zeta z \left| \begin{array}{c} \left(a_2, \frac{2}{\alpha_2}\right), (0, 1) \\ \left(b_3, \frac{2}{\alpha_1}\right), (1, 1) \end{array} \right. \right], \quad (16)$$

where  $a_2 = \mu_2 + v$ , and the MGF of  $Z$  follows from [41, Eq. 2.19] and given as

$$M_Z(s) = \theta_1 \theta_2 \sum_{u,v=0}^{\infty} A_{u,v} H_{1,1}^{1,1} \left[ \frac{\zeta}{(-s)} \left| \begin{array}{c} (1, 1), \left(a_2, \frac{2}{\alpha_2}\right) \\ \left(b_3, \frac{2}{\alpha_1}\right) \end{array} \right. \right]. \quad (17)$$

### A. Higher Moments of $Z$

Unlike the case of product statistics, the  $n$ -th order moment of RV  $Z$ , *i.e.*,  $\mathbb{E}[Z^n] \neq \frac{\mathbb{E}[X_1^n]}{\mathbb{E}[X_2^n]}$  even though the  $X_1$  and  $X_2$  are independent. But, the Mellin transform can be used as  $\mathbb{E}[Z^n] = \mathcal{M}[f_Z(z); s]|_{s=n+1}$ . Hence, from (13) we have

$$\begin{aligned} \mathbb{E}[Z^n] &= \theta_1 \theta_2 (\bar{\gamma}_1)^n (\bar{\gamma}_2)^{-n} c_1^{\frac{2n}{\alpha_1}} c_2^{\frac{-2n}{\alpha_2}} \Gamma\left(\mu_1 + \frac{2n}{\alpha_1}\right) \\ &\times \Gamma\left(\mu_2 - \frac{2n}{\alpha_2}\right) {}_2F_1\left(m_1, \mu_1 + \frac{2n}{\alpha_1}; \mu_1; \beta_1\right) \\ &\times {}_2F_1\left(m_2, \mu_2 - \frac{2n}{\alpha_2}; \mu_2; \beta_2\right). \end{aligned} \quad (18)$$

## V. INTEGRAL REPRESENTATION

In the previous sections, we have derived the expressions for the PDF of the product and ratio statistics of two i.n.i.d.  $\alpha - \kappa - \mu$  shadowed RVs. However, the expression in (7), and (15) involves the H-function, which is not implemented in popular software like *MATLAB*. The H-function is available in *Mathematica* and can be used to evaluate the derived expression. Still, due to the presence of double infinite summation and considering the general nature of the values of the parameter involved, it is difficult to predict the number of terms to add for a particular level of accuracy.

In this section, we have given the Laplace type integral representation for the derived expression using the method of residue and the definition of the Gamma function. These real-integral type expressions are far easier to evaluate using the Gauss-Legendre quadrature rule than evaluating a double infinite series with an H-function.

### A. Laplace type integral for the PDF of the product statistics

By substituting the definition of H-function in (7), we have

$$f_Y(y) = \delta\theta_1\theta_2 \sum_{u,v=0}^{\infty} \frac{A_{u,v}}{2\pi i} \int_C \Gamma\left(\mu_1 + u - \frac{2}{\alpha_1} + \frac{2}{\alpha_1}s\right) \times \Gamma\left(\mu_2 + v - \frac{2}{\alpha_2} + \frac{2}{\alpha_2}s\right) (\delta y)^{-s} ds \quad (19)$$

Let  $\mu_1 + u - \frac{2}{\alpha_1} + \frac{2}{\alpha_1}s = \omega$  then,  $f_Y(y)$  can be written as

$$f_Y(y) = \frac{\alpha_1\theta_1\theta_2\delta(\beta_3)^{\mu_1 - \frac{2}{\alpha_1}}}{2} \sum_{u,v=0}^{\infty} \frac{A_{u,v}\beta_3^u}{2\pi i} \int_C \Gamma(\omega) \times \Gamma\left(\mu_2 - \frac{\alpha_1}{\alpha_2}\mu_1 - \frac{\alpha_1}{\alpha_2}u + v + \frac{\alpha_1}{\alpha_2}\omega\right) \beta_3^{-\omega} d\omega, \quad (20)$$

where  $\beta_3 = (\delta y)^{\frac{\alpha_1}{2}}$ . From [42, Eq. 4] the Mellin-Barnes integral in the above equation can be identified as the Krätzel function. Hence, we have

$$f_Y(y) = \frac{\alpha_2\theta_1\theta_2\delta(\beta_3)^{\mu_1 - \frac{2}{\alpha_1}}}{2} \sum_{u,v=0}^{\infty} A_{u,v}\beta_3^u Z_\rho^\nu(\beta_3), \quad (21)$$

$$f_Z(z) = \begin{cases} \frac{\alpha_1 \zeta \theta_1 \theta_2 (\beta_5)^{\mu_1 - \frac{2}{\alpha_1}}}{2} \int_0^\infty t^{(\mu_2 + \frac{\alpha_1}{\alpha_2} \mu_1 - 1)} e^{-t} {}_1F_1\left(m_1; \mu_1; t^{\frac{\alpha_1}{\alpha_2}} \beta_1 \beta_5\right) {}_1F_1\left(m_2; \mu_2; t \beta_2\right) e^{-\beta_5 t^{\frac{\alpha_1}{\alpha_2}}} dt & \text{for } \zeta z < 1, \\ \frac{\alpha_2 \zeta \theta_1 \theta_2 (\beta_6)^{\mu_2 + \frac{2}{\alpha_2}}}{2} \int_0^\infty t^{(\mu_1 + \frac{\alpha_2}{\alpha_1} \mu_2 - 1)} e^{-t} {}_1F_1\left(m_1; \mu_1; t \beta_1\right) {}_1F_1\left(m_2; \mu_2; t^{\frac{\alpha_2}{\alpha_1}} \beta_2 \beta_6\right) e^{-\beta_6 t^{\frac{\alpha_2}{\alpha_1}}} dt & \text{for } \zeta z > 1, \end{cases} \quad (24)$$

where  $\beta_5 = (\zeta z)^{\frac{\alpha_1}{2}}$ , and  $\beta_6 = (\zeta z)^{-\frac{\alpha_2}{2}}$ .

where  $\rho = \frac{\alpha_2}{\alpha_1}$ ,  $\nu = \frac{\alpha_2}{\alpha_1}(\mu_2 + v) - \mu_1 - u$  and  $Z_\rho^\nu(\cdot)$  is the Krätzel function. Next, using the definition on Krätzel function [42, Eq. 1] and some algebraic manipulation, a single Laplace type integral representation of  $f_Y(y)$  is

$$f_Y(y) = \frac{\alpha_1 \theta_1 \theta_2 \delta (\beta_3)^{\mu_1 - \frac{2}{\alpha_1}}}{2} \int_0^\infty t^{(\mu_2 - \frac{\alpha_1}{\alpha_2} \mu_1 - 1)} e^{-t} \times {}_1F_1\left(m_1; \mu_1; t^{-\frac{\alpha_1}{\alpha_2}} \beta_1 \beta_3\right) {}_1F_1\left(m_2; \mu_2; t \beta_2\right) \times e^{-\beta_3 t^{-\frac{\alpha_1}{\alpha_2}}} dt. \quad (22)$$

### B. Laplace type integral for the PDF of the ratio statistics

Using the calculus of residues, the series form of PDF in (15) is as follows

$$f_Z(z) = \begin{cases} \frac{\alpha_1 \zeta \theta_1 \theta_2}{2} \sum_{u,v,n=0}^{\infty} \frac{A_{u,v}(-1)^n}{n!} \times \Gamma\left(\mu_2 + \frac{\alpha_1}{\alpha_2} \mu_1 + \frac{\alpha_1}{\alpha_2} u + v + \frac{\alpha_1}{\alpha_2} n\right) (\zeta z)^{\frac{\alpha_1(b_1+n)}{2}} & \text{for } \zeta z < 1 \\ \frac{\alpha_2 \zeta \theta_1 \theta_2}{2} \sum_{u,v,n=0}^{\infty} \frac{A_{u,v}(-1)^n}{n!} \times \Gamma\left(\mu_1 + \frac{\alpha_2}{\alpha_1} \mu_2 + u + \frac{\alpha_2}{\alpha_1} v + \frac{\alpha_2}{\alpha_1} n\right) \left(\frac{1}{\zeta z}\right)^{\frac{\alpha_2(1-a_1+n)}{2}} & \text{for } \zeta z > 1 \end{cases} \quad (23)$$

Next, using the definition of the Gamma function and some algebraic manipulations, the Laplace type integral for the ratio statistics is given by (24) on the top of the next page. Note that ratio RV can be used to model the signal-to-interference ratio between the desired user and the interference user. Since both the users are present in the same propagation environment, it is practical to

assume  $\alpha_1 = \alpha_2 = \alpha$ . For this special case, it is easy to show that  $H_{1,1}^{1,1} \left[ \zeta z \left| \begin{matrix} (a_1, \frac{2}{\alpha}) \\ (b_1, \frac{2}{\alpha}) \end{matrix} \right. \right] =$

$\frac{\alpha\Gamma(1-a_1+b_1)}{2} \frac{(\zeta z)^{\frac{\alpha b_1}{2}}}{(1+(\zeta z)^{\frac{\alpha}{2}})^{1-a_1+b_1}}$ . After substituting this in (15) and some algebraic manipulations, we have

$$f_Z(z) = \frac{\alpha\zeta\theta_1\theta_2(\beta_7)^{\mu_1-\frac{2}{\alpha}}}{2(1+\beta_7)^{\mu_1+\mu_2}} \int_0^\infty t^{(\mu_1+\mu_2-1)} e^{-t} \times {}_1F_1\left(m_1; \mu_1; \frac{t\beta_1\beta_7}{1+\beta_7}\right) {}_1F_1\left(m_2; \mu_2; \frac{t\beta_2}{1+\beta_7}\right) dt, \quad (25)$$

where  $\beta_7 = (\zeta z)^{\frac{\alpha}{2}}$ . The above integral can be identified as a double hypergeometric series (Appell series)  $F_2$  [39, 1.3.3], and we have

$$f_Z(z) = \frac{\alpha\zeta\theta_1\theta_2\Gamma(\mu_1+\mu_2)(\beta_7)^{\mu_1-\frac{2}{\alpha}}}{2(1+\beta_7)^{\mu_1+\mu_2}} \times F_2\left(\mu_1+\mu_2, m_1, m_2; \mu_1, \mu_2; \frac{\beta_1\beta_7}{1+\beta_7}, \frac{\beta_2}{1+\beta_7}\right) \quad (26)$$

## VI. ASYMPTOTIC ANALYSIS

In previous section, we derived the exact Laplace type integral expressions for the PDF of the product and ratio statistics of two i.n.i.d.  $\alpha - \kappa - \mu$  shadowed RVs. In order to get more insight and simplified expression, we focused on the asymptotic analysis in this section.

### A. For the Product Statistics

In high SNR regime, when either or both  $\bar{\gamma}_1, \bar{\gamma}_2 \rightarrow \infty$ . We have  $\beta_3 \rightarrow 0$ . The PDF of the product statistics in (22) simplifies to

$$f_Y(y) |_{\uparrow} \approx \frac{\alpha_1\theta_1\theta_2\delta(\beta_3)^{\mu_1-\frac{2}{\alpha_1}}}{2} \int_0^\infty t^{(\mu_2-\frac{\alpha_1}{\alpha_2}\mu_1-1)} e^{-t} \times {}_1F_1(m_2; \mu_2; t\beta_2) dt. \quad (27)$$

Using the identity [43, 7.621.4], we have

$$f_Y(y) |_{\uparrow} \approx \frac{\alpha_1\theta_1\theta_2\delta(\beta_3)^{\mu_1-\frac{2}{\alpha_1}}}{2} \Gamma\left(\mu_2 - \frac{\alpha_1}{\alpha_2}\mu_1\right) \times {}_2F_1\left(m_2, \mu_2 - \frac{\alpha_1}{\alpha_2}\mu_1; \mu_2; \beta_2\right). \quad (28)$$

Hence, in high SNR regime, asymptotic CDF of the product statistics can be approximated as

$$F_Y(y) |_{\uparrow} \approx \frac{\theta_1\theta_2}{\mu_1} \Gamma\left(\mu_2 - \frac{\alpha_1}{\alpha_2}\mu_1\right) \times {}_2F_1\left(m_2, \mu_2 - \frac{\alpha_1}{\alpha_2}\mu_1; \mu_2; \beta_2\right) \beta_3^{\mu_1}. \quad (29)$$

### B. For the Ratio Statistics

When  $\bar{\gamma}_1 \rightarrow \infty$ , we have  $\beta_5 \rightarrow 0$ . The PDF of the ratio statistics in (24) simplifies to

$$\begin{aligned}
 f_Z(z) \Big|_{\uparrow} &= \frac{\alpha_1 \theta_1 \theta_2 \zeta(\beta_5)^{\mu_1 - \frac{2}{\alpha_1}}}{2} \int_0^\infty t^{\left(\mu_2 + \frac{\alpha_1}{\alpha_2} \mu_1 - 1\right)} e^{-t} \\
 &\quad \times {}_1F_1\left(m_2; \mu_2; t\beta_2\right) dt, \\
 &= \frac{\alpha_1 \theta_1 \theta_2 \zeta(\beta_5)^{\mu_1 - \frac{2}{\alpha_1}}}{2} \Gamma\left(\mu_2 + \frac{\alpha_1}{\alpha_2} \mu_1\right) \\
 &\quad \times {}_2F_1\left(m_2, \mu_2 + \frac{\alpha_1}{\alpha_2} \mu_1; \mu_2; \beta_2\right)
 \end{aligned} \tag{30}$$

Hence, the asymptotic approximation for the CDF of the ratio statistics is

$$\begin{aligned}
 F_Z(z) \Big|_{\uparrow} &= \frac{\theta_1 \theta_2}{\mu_1} \Gamma\left(\mu_2 + \frac{\alpha_1}{\alpha_2} \mu_1\right) \\
 &\quad \times {}_2F_1\left(m_2, \mu_2 + \frac{\alpha_1}{\alpha_2} \mu_1; \mu_2; \beta_2\right) \beta_5^{\mu_1}
 \end{aligned} \tag{31}$$

## VII. SIMPLE APPROXIMATION

Although the expressions, derived for the PDF of product and ratio statistics of two  $\alpha - \kappa - \mu$  shadowed RVs in (22) and (24), are exact and easy to evaluate numerically. For some practical applications, having a simpler approximation for the PDF is helpful, as it helps to analyze and make inferences for complex systems. Hence, we proposed the Gamma distribution as a closed-form approximation for the product and the Beta prime distribution as a closed-form approximation for the ratio of two  $\alpha - \kappa - \mu$  shadowed RVs. The parameters of respective distributions can be obtained using the method of moments.

### A. Gamma Approximation for Product Statistics

We have  $Y = X_1 X_2$ , where  $X_1$  and  $X_2$  follows  $\alpha - \kappa - \mu$  shadowed distribution. The first two moments of  $Y$  are evaluated using (12) and are as follows

$$\begin{aligned}
 \mathbb{E}[Y] &= \bar{\gamma}_1 \bar{\gamma}_2, \\
 \mathbb{E}[Y^2] &= \theta_1 \theta_2 (\bar{\gamma}_1 \bar{\gamma}_2)^2 c_1^{\frac{4}{\alpha_1}} c_2^{\frac{4}{\alpha_2}} \Gamma\left(\mu_1 + \frac{4}{\alpha_1}\right) \\
 &\quad \times \Gamma\left(\mu_2 + \frac{4}{\alpha_2}\right) {}_2F_1\left(m_1, \mu_1 + \frac{4}{\alpha_1}; \mu_1; \beta_1\right) \\
 &\quad \times {}_2F_1\left(m_2, \mu_2 + \frac{4}{\alpha_2}; \mu_2; \beta_2\right)
 \end{aligned} \tag{32}$$

Let  $G(k, \theta)$  represents the Gamma distribution with shape parameter  $k$  and scale parameter  $\theta$ . The PDF of  $Y$  is approximated as

$$f_Y(y) = \frac{y^{k_Y-1} e^{-\frac{y}{\theta_Y}}}{\Gamma(k_Y) \theta_Y^{k_Y}} \quad y > 0, \quad (33)$$

where  $k, \theta$  are related to moments of  $W$  in the following manner

$$k_Y = \frac{\mathbb{E}[Y]}{\theta}, \quad \theta_Y = \frac{\mathbb{V}[Y]}{\mathbb{E}[Y]}. \quad (34)$$

The parameter for approximating Gamma distribution can be evaluated as follows

$$k_Y = \frac{1}{C_{pro}}, \quad \theta_Y = \bar{\gamma}_1 \bar{\gamma}_2 C_{pro}, \quad (35)$$

where  $C_{pro} = \theta_1 \theta_2 c_1^{\frac{4}{\alpha_1}} c_2^{\frac{4}{\alpha_2}} \Gamma\left(\mu_1 + \frac{4}{\alpha_1}\right) \Gamma\left(\mu_2 + \frac{4}{\alpha_2}\right) {}_2F_1\left(m_1, \mu_1 + \frac{4}{\alpha_1}; \mu_1; \beta_1\right) {}_2F_1\left(m_2, \mu_2 + \frac{4}{\alpha_2}; \mu_2; \beta_2\right) - 1$ .

### B. Beta prime Approximation for Ratio Statistics

We have  $Z = \frac{X_1}{X_2}$ , where  $X_1$  and  $X_2$  follows  $\alpha - \kappa - \mu$  shadowed distribution. Similar to [35], we first approximated the  $X_1$  and  $X_2$  by a Gamma random variable using moment matching. Let  $X_1 \sim G(k_{Z1}, \theta_{Z1})$  and  $X_2 \sim G(k_{Z2}, \theta_{Z2})$ , where  $k_{Z1}, \theta_{Z1}, k_{Z2}, \theta_{Z2}$  are calculated as follows

$$k_{Z1} = \frac{1}{C_{ratio}}, \quad \theta_{Z1} = \bar{\gamma}_1 C_{ratio}, \quad (36)$$

where  $C_{ratio} = \theta_1 c_1^{\frac{4}{\alpha_1}} \Gamma\left(\mu_1 + \frac{4}{\alpha_1}\right) {}_2F_1\left(m_1, \mu_1 + \frac{4}{\alpha_1}; \mu_1; \beta_1\right) - 1$  and

$$k_{Z2} = \frac{1}{D_{ratio}}, \quad \theta_{Z2} = \bar{\gamma}_2 D_{ratio}, \quad (37)$$

where  $D_{ratio} = \theta_2 c_2^{\frac{4}{\alpha_2}} \Gamma\left(\mu_2 + \frac{4}{\alpha_2}\right) {}_2F_1\left(m_2, \mu_2 + \frac{4}{\alpha_2}; \mu_2; \beta_2\right) - 1$ . Under the assumption that  $X_1$  and  $X_2$  follows Gamma distribution,  $Z$  can be approximated by beta prime distribution [44]. The PDF of  $Z$  is approximated as

$$f_Z(z) = \frac{\frac{\theta_{Z2}}{\theta_{Z1}} \left(\frac{\theta_{Z2}}{\theta_{Z1}} z\right)^{k_{Z1}-1}}{B(k_{Z1}, k_{Z2}) \left(1 + \frac{\theta_{Z2}}{\theta_{Z1}} z\right)^{k_{Z1}+k_{Z2}}} \quad z > 0, \quad (38)$$

where  $B(\cdot, \cdot)$  is the Beta function [45]. Next, we have compared the proposed close-form approximations with simulated numerical values. In Fig. 1 and 2, we have plotted the approximated and simulated PDF of  $Y$  and  $Z$ , respectively for  $\alpha_1 = 1.5, \kappa_1 = 5.0, \mu_1 = 1.2$  and  $\alpha_2 = 2.5, \kappa_2 = 2.1, \mu_2 = 3.0$  with different values of  $m_1$  and  $m_2$ .

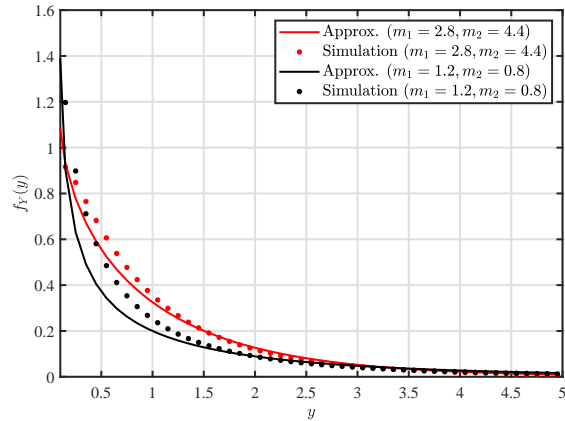


Fig. 1: Simulated and Approximate PDF of  $Y$

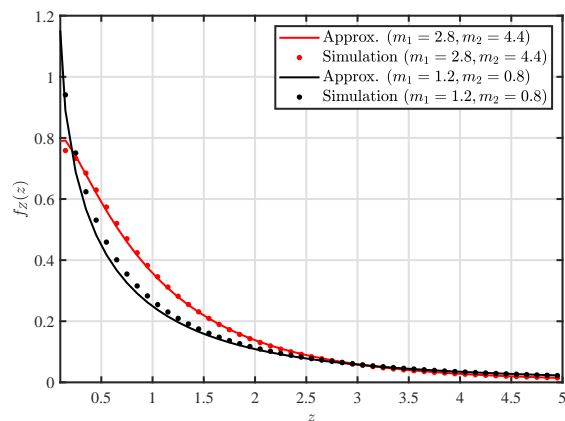


Fig. 2: Simulated and Approximate PDF of  $Z$

Fig. 1 and 2 shows that the proposed approximation are close to the simulated values of PDF and can be used in order to get a simplified expression in practical applications.

In the next section, we discuss some applications where the product and ratio statistics of two  $\alpha - \kappa - \mu$  shadowed EV are useful.

## VIII. APPLICATION EXAMPLES

### A. Cascaded Wireless System

Consider a two-tap cascaded channel where both taps follow  $\alpha - \kappa - \mu$  shadowed fading. The considered model is a generalization of many existing works in literature such as [24]–[26]. This section derives the analytical expression for various important metrics for such a system.

1) *Outage Probability*: In any communication system, an outage is when the signal's received strength falls below a certain threshold. The outage probability (OP) is defined as  $P_{OP}(\gamma_{th}) = \mathbb{P}(Y \leq \gamma_{th})$ , hence, we have

$$P_{OP}(\gamma_{th}) = \theta_1 \theta_2 \sum_{u,v=0}^{\infty} A_{u,v} \times H_{1,3}^{2,1} \left[ \delta \gamma_{th} \left| \begin{matrix} (0, 1) \\ \left(b_3, \frac{2}{\alpha_1}\right), \left(b_4, \frac{2}{\alpha_2}\right), (1, 1) \end{matrix} \right. \right] \quad (39)$$

where  $b_3 = \mu_1 + u, b_4 = \mu_2 + v$ . Apart from using this double-infinite series expression, we can also make use of (22) to compute the OP as  $P_{OP}(\gamma_{th}) = \int_0^{\gamma_{th}} f_Y(y) dy$ . This integral can be evaluated using the Gauss-Legendre quadrature rule [46, 25.4.29].

2) *Amount of Fading*: The amount of fading (AF) measures the severity of any fading channel. It is defined as the ratio of variance to the square of the mean of instantaneous SNR [47]. Hence, the AF for cascaded  $\alpha - \kappa - \mu$  shadowed channel is

$$\text{AF} = \frac{\mathbb{V}[Y]}{(\mathbb{E}[Y])^2} = \frac{\mathbb{E}[Y^2] - (\mathbb{E}[Y])^2}{(\mathbb{E}[Y])^2}. \quad (40)$$

The AF can now be calculated using (12).

**Remark:** For  $\alpha_1 = \alpha_2 = 2$  the result in (39) coincides with the corresponding result in [26]. Similarly, for  $\alpha_i = 2, m_i \rightarrow \infty$ , our OP and AF expression reduces to the [24, Eq. (20)] and [24, Eq. (16)], respectively. In [25], the cascade channel with  $\alpha - \mu, \kappa - \mu$ , and  $\eta - \mu$  fading are considered since these three fading models are the special case of  $\alpha - \kappa - \mu$  shadowed fading hence, the results encompass the corresponding results in [25].

## B. Physical Layer Security

In [33]–[35], [48] instantaneous secrecy capacity of typical 3 node single-input-single-output (SISO) wireless communication system is defined as

$$C_S = [\log_2(1 + \gamma_{SD}) - \log_2(1 + \gamma_{SE})]^+ \quad (41)$$

where  $[x]^+ = \max\{x, 0\}$ . The  $\gamma_{SD}$  and  $\gamma_{SE}$  are instantaneous SNR over the source to legitimate destination and source to eavesdropper link, respectively. Both links are assumed to be experiencing  $\alpha - \kappa - \mu$  shadowed fading. The secrecy outage probability (SOP) is defined as the phenomenon in which the instantaneous secrecy capacity falls below a certain target secrecy rate  $R_S$ , i.e., we have

$$P_{SOP}(R_S) = \mathbb{P}[C_S \leq R_S] \quad (42)$$

Using [32],  $P_{SOP}(R_s)$  is simplified as

$$P_{SOP}(R_s) = \mathbb{P} \left[ \frac{1 + \gamma_{SD}}{1 + \gamma_{SE}} \leq \gamma_{th} \right] \quad (43)$$

where  $\gamma_{th} = 2^{R_s}$ . Applying the approximation  $\frac{1+x}{1+y} \approx \frac{x}{y}$  [49], we have

$$P_{SOP}(R_s) \approx \mathbb{P} \left[ \frac{\gamma_{SD}}{\gamma_{SE}} \leq \gamma_{th} \right] \quad (44)$$

The above equation is nothing but the CDF of the ratio of two  $\alpha - \kappa - \mu$  shadowed RVs, that is given in (16). Another secrecy performance metric is strictly positive secrecy capacity (SPSC) which is defined as  $P_0 = \mathbb{P}[C_s > 0]$ . In terms of SOP, we can write SPSC as  $P_0 = 1 - P_{SOP}(0)$ .

**Remark:** Recently, the authors in [29] studied the secrecy performance under  $\alpha - \kappa - \mu$  shadowed fading, but the results are valid only for integer values of  $\mu_1$  and  $\mu_2$ . Whereas the results derived in this paper have no such restriction. Since the  $\alpha - \kappa - \mu$  shadowed fading is the general case for other fading scenarios such as Nakagami- $m$ ,  $\kappa - \mu$ ,  $\kappa - \mu$  shadowed hence, our results for SOP and SPSC encompasses the results in [32]–[35].

### C. IRS-Assisted Communication System

Considering a system model similar to [23], we have one single antenna source node (**S**) communicating with one single antenna destination node (**D**) using an IRS with  $N$  reflector elements. Let,  $\mathbf{h}^{SR} \in \mathbb{C}^{N \times 1}$ ,  $\mathbf{h}^{RD} \in \mathbb{C}^{N \times 1}$  and  $h^{SD} \in \mathbb{C}^1$  denote the small-scale fading channel coefficients of the **S** to IRS (SR), IRS to **D** (RD) and **S** to **D** (SD) link, respectively. All the channels are assumed to experience independent  $\alpha - \kappa - \mu$  shadowed fading *i.e.*, each of  $|\mathbf{h}^{SR}_i|^2$ ,  $|\mathbf{h}^{RD}_i|^2$  and  $|h^{SD}|^2$  has the PDF as given in (2) with  $\mathbb{E} \left[ |\mathbf{h}^{AB}_i|^2 \right] = \gamma_{AB} = d_{AB}^{-\beta}$  where  $A, B \in \{S, R, D\}$ . The  $d_{AB}$  represents the distance between node  $A, B$ , and  $\beta$  is the path-loss coefficient. Let  $\theta_i = \arg(h^{SD}) - \arg([\mathbf{h}^{SR}]_i [\mathbf{h}^{RD}]_i)$  be the phase shift introduced by the  $i$ -th IRS element. This phase-shift design is widely used in IRS literature, such as [23], [50]–[52]. Then the SNR at the node **D** is

$$\gamma_{IRS} = \gamma_s \left| h^{SD} + \sum_{i=1}^N [\mathbf{h}^{SR}]_i [\mathbf{h}^{RD}]_i \right|^2, \quad (45)$$

where  $\gamma_s$  is the ratio of transmitted power  $p$  and receiver noise power  $\sigma^2$ . In any communication system, an outage is when the signal's received strength falls below a certain threshold. Let

$|h^{SD}|$ ,  $|\mathbf{h}^{SR}]_i|$  and  $|\mathbf{h}^{RD}]_i|$  be denoted by  $g^{SD}$ ,  $[\mathbf{g}^{SR}]_i$  and  $[\mathbf{g}^{RD}]_i$  respectively. The outage probability (OP) for threshold  $\gamma_{th}$  can be evaluated as

$$\begin{aligned} P_{out}(\gamma_{th}) &= \mathbb{P} \left( \gamma_s \left| \left( g^{SD} + \underbrace{\sum_{i=1}^N [\mathbf{g}^{SR}]_i [\mathbf{g}^{RD}]_i}_u \right) \right|^2 \leq \gamma_{th} \right) \\ &= \mathbb{P} \left( z \leq \sqrt{\frac{\gamma_{th}}{\gamma_s}} \right), \end{aligned} \quad (46)$$

where  $z \triangleq u + g^{SD}$ . Now approximate the  $u$  by the Gamma RV, i.e.,  $u \sim G(k_{mom}, \theta_{mom})$  with

$$k_{mom} = \frac{N\mu^2}{\sigma^2}, \quad \theta_{mom} = \frac{\sigma^2}{\mu}, \quad (47)$$

where  $\mu$ , and  $\sigma^2$  are evaluated using (12) as follows

$$\begin{aligned} \mu &= \theta_{SR}\theta_{RD} (\bar{\gamma}_{SR}\bar{\gamma}_{RD})^{0.5} c_{SR}^{\frac{1}{\alpha_{SR}}} c_{RD}^{\frac{1}{\alpha_{RD}}} \Gamma \left( \mu_{SR} + \frac{1}{\alpha_{SR}} \right) \\ &\times \Gamma \left( \mu_{RD} + \frac{1}{\alpha_{RD}} \right) {}_2F_1 \left( m_{SR}, \mu_{SR} + \frac{1}{\alpha_{SR}}; \mu_{SR}; \beta_{SR} \right) \\ &\times {}_2F_1 \left( m_{RD}, \mu_{RD} + \frac{1}{\alpha_{RD}}; \mu_{RD}; \beta_{RD} \right), \end{aligned} \quad (48)$$

and the  $\sigma^2 = \bar{\gamma}_{SR}\bar{\gamma}_{RD} - \mu^2$ . The  $z$  is a sum of two independent RV, so the CDF of the  $z$  is as follows

$$F_z(z) = \int_{-\infty}^{\infty} f_u(z-x) F_{g^{SD}}(x) dx, \quad (49)$$

where  $f_u(x) = \frac{1}{\Gamma(k_{mom})\theta_{mom}^{k_{mom}}} x^{k_{mom}-1} e^{-\frac{x}{\theta_{mom}}}$  is the pdf of  $u$  and  $F_{g^{SD}}(x)$  is the CDF of  $g^{SD}$ .

After substituting values, we have

$$\begin{aligned} F_z(z) &= \frac{\theta_{SD}}{\mu_{SD} c_{SD}^{\mu_{SD}} \Gamma(k_{mom}) \theta_{mom}^{k_{mom}}} \int_0^z (z-x)^{k_{mom}-1} \\ &\times e^{-\frac{z-x}{\theta_{mom}}} (\lambda(x))^{\mu_{SD}} \\ &\times \Phi_2 \left( \mu_{SD} - m_{SD}, m_{SD}; \mu_{SD} + 1; \right. \\ &\quad \left. \frac{-\lambda(x)}{c_{SD}}, -\lambda(x) \frac{1 - \beta_{SD}}{c_{SD}} \right) dx, \end{aligned} \quad (50)$$

where  $\Phi_2(\cdot, \cdot; \cdot; \cdot, \cdot)$  is the confluent bivariate hypergeometric function [39],  $\lambda(x) = \left( \frac{x^2}{\bar{\gamma}_{SD}} \right)^{\frac{\alpha_{SD}}{2}}$ .

Let  $\frac{z-x}{\theta_{mom}} = t \Rightarrow dx = -\theta_{mom} dt$  then, OP is given by (51) on the top of next page.

$$\begin{aligned}
P_{out}(\gamma_{th}) &\approx \frac{\theta_{SD}}{\mu_{SD} c_{SD}^{\mu_{SD}} \Gamma(k_{mom})} \int_0^{\sqrt{\frac{\gamma_{th}}{\gamma_s}}} t^{k_{mom}-1} e^{-t} \left( \lambda \left( \sqrt{\frac{\gamma_{th}}{\gamma_s}} - t\theta_{mom} \right) \right)^{\mu_{SD}} \\
&\times \Phi_2 \left( \mu_{SD} - m_{SD}, m_{SD}; \mu_{SD} + 1; \frac{-\lambda \left( \sqrt{\frac{\gamma_{th}}{\gamma_s}} - t\theta_{mom} \right)}{c_{SD}}, -\lambda \left( \sqrt{\frac{\gamma_{th}}{\gamma_s}} - t\theta_{mom} \right) \frac{1 - \beta_{SD}}{c_{SD}} \right) dt
\end{aligned} \tag{51}$$

$$\begin{aligned}
P_{out}(\gamma_{th}) &\approx \frac{\theta_{SD}}{\mu_{SD} c_{SD}^{\mu_{SD}} \sqrt{\pi}} \int_{\frac{N\mu - \sqrt{\frac{\gamma_{th}}{\gamma_s}}}{\sqrt{2N\sigma^2}}}^{\infty} \exp(-t^2) (h(t))^{\mu_{SD}} \\
&\times \Phi_2 \left( \mu_{SD} - m_{SD}, m_{SD}; \mu_{SD} + 1; \frac{-h(t)}{c_{SD}}, -h(t) \frac{1 - \beta_{SD}}{c_{SD}} \right) dt
\end{aligned} \tag{52}$$

For the large values of  $k_{mom}$ , the expression in (51) can be numerically unstable due to the presence of  $\Gamma(k_{mom})$ . In such case, we can use a widely known fact in statistics that, for large  $k_{mom}$ , a Gamma RV is approximated via Gaussian RV [53]. Using the Gaussian approximation for  $u$ , OP for threshold  $\gamma_{th}$  is given in (52) on the top of next page, where  $h(t) = \lambda \left( \frac{t}{\sqrt{2N\sigma^2}} - \frac{N\mu - \sqrt{\frac{\gamma_{th}}{\gamma_s}}}{\sqrt{2N\sigma^2}} \right)$ . The utility of (51) and (52) is demonstrated in Section IX. Note that the confluent bivariate hypergeometric function  $\Phi_2$  is not implemented in *MATLAB*. However, a *MATLAB* program for the evaluation of  $\Phi_2$  is given in [54] that is used in the evaluation of (51) and (52).

**Remark:** The results derived here are quite general and encompass many previous results in the literature as special cases. For example, the (52) reduces to [36, Theorem 2] when SD link is Rayleigh distributed, SR and RD link are Rician distributed, *i.e.*  $\alpha_{SD} = 2, \kappa_{SD} = 0, \mu_{SD} = 1, m_{SD} \rightarrow \infty$  and  $\alpha_{SR} = \alpha_{RD} = 2, \kappa_{SR} = K_1, \kappa_{RD} = K_2, \mu_{SR} = \mu_{RD} = 1, m_{SR}, m_{RD} \rightarrow \infty$ . Similarly, the OP expression given in [37, Eq. (10)] and [38, Eq. (15)] are special cases when the SD link is in the outage, and the SR, RD link follows Rayleigh distribution. Similarly, the derived results generalize the work in [22], [23] for no phase error case.

## IX. NUMERICAL RESULTS

This section presents the simulation results that show the correctness and utility of the theoretical expression presented in the previous sections. Without loss of generality, we have

assumed  $\bar{\gamma}_1 = \bar{\gamma}_2 = 1$  for all the plots, unless mentioned otherwise. In all the figures, we have used solid lines to draw the theoretical values and the dotted markers are for simulated values. In Figs. 3 and 4, several plots for the product PDF of two  $\alpha - \kappa - \mu$  shadowed RV for various values of  $\alpha, \kappa, \mu$  and  $m$  are given. In Fig. 3(a), we have plotted PDF of product of two  $\alpha - \kappa - \mu$  shadowed RVs with  $\kappa_1 = 5.0, \mu_1 = 1.2, m_1 = 2.8$  and  $\kappa_2 = 2.1, \mu_2 = 3.0, m_2 = 4.4$  for different combination of  $\alpha_1$  and  $\alpha_2$  values. Similarly, in Fig. 3(b), we have plotted the PDF of  $Y$  for different combination of  $\kappa_1$  and  $\kappa_2$  values with  $\alpha_1 = 1.5, \mu_1 = 2.1, m_1 = 10.0$  and  $\alpha_2 = 2.5, \mu_2 = 1.5, m_2 = 4.0$ . Next, we have plotted the PDF of  $Y$  for different combinations of  $\mu$  and  $m$  in Fig. 4. Particularly, in Fig. 4(a) for  $\alpha_1 = 1.0, \kappa_1 = 2.2, m_1 = 10.0$  and  $\alpha_2 = 1.5, \kappa_2 = 0.9, m_2 = 4.0$ , the plots are given for different combination of  $\mu_1$  and  $\mu_2$ . Lastly, Fig. 4(b) has the results for different combination of  $m_1$  and  $m_2$  with  $\alpha_1 = 1.5, \kappa_1 = 5.0, \mu_1 = 1.2$  and  $\alpha_2 = 2.5, \kappa_2 = 2.1, \mu_2 = 3.0$ . Hence, one can observe that a wide range of shapes can be fitted through double  $\alpha - \kappa - \mu$  shadowed RV. Also, note that the simulated PDFs are perfectly matching with the values obtained through theoretical expression in (22), which shows the correctness and utility of expression.

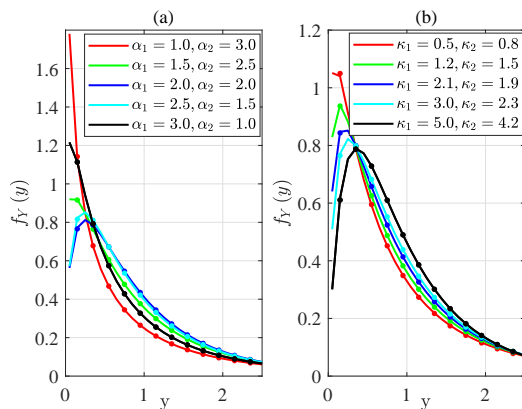


Fig. 3: PDF of  $Y$  for various values of  $\alpha_1, \alpha_2$  in (a), and for various values of  $\kappa_1, \kappa_2$  in (b).

Next, We plotted the PDF values for the ratio of two  $\alpha - \kappa - \mu$  shadowed RVs in Figs. 5 and 6. The parameters values in Fig. 5(a) and (b) are the same as kept for Fig. 3(a) and (b). Similar is the case with Fig. 6(a),(b) and Fig. 4(a),(b). In all the plots, the value of PDF obtained through simulated RV and theoretical expression in (24) and (26).

In the following subsections, we have presented the simulation results for the applications discussed in Section VIII.

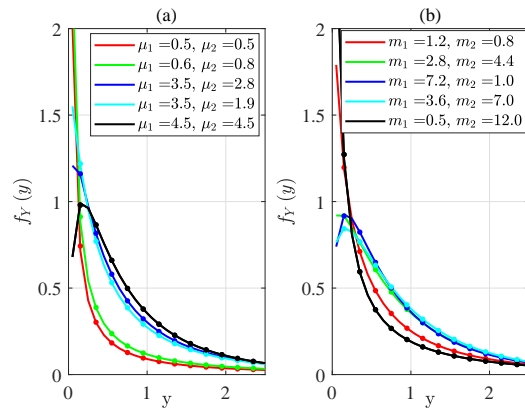


Fig. 4: PDF of  $Y$  for various values of  $\mu_1, \mu_2$  in (a), and for various values of  $m_1, m_2$  in (b).

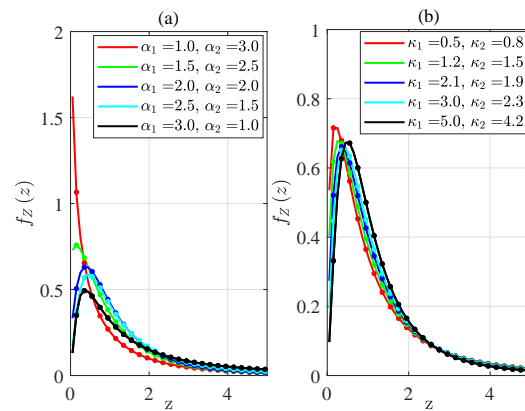


Fig. 5: PDF of  $Z$  for various values of  $\alpha_1, \alpha_2$  in (a), and for various values of  $\kappa_1, \kappa_2$  in (b).

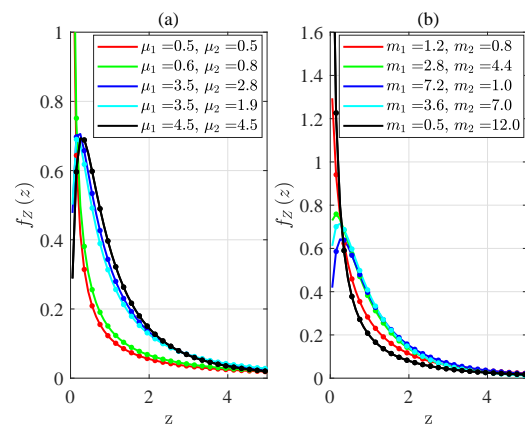


Fig. 6: PDF of  $Z$  for various values of  $\mu_1, \mu_2$  in (a), and for various values of  $m_1, m_2$  in (b).

### A. Results for Cascaded Wireless System

This subsection presents the OP and AF for a cascaded wireless system over  $\alpha - \kappa - \mu$  shadowed fading. Fig. 7 and 8 show the impact of  $\alpha$  parameter on OP and AF, respectively, while other parameters are kept constant.

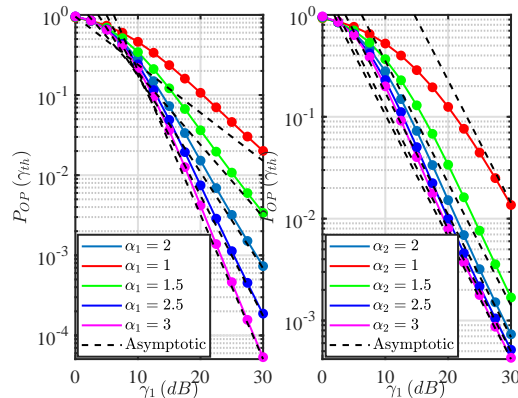


Fig. 7: OP of cascaded  $\alpha - \kappa - \mu$  shadowed channel

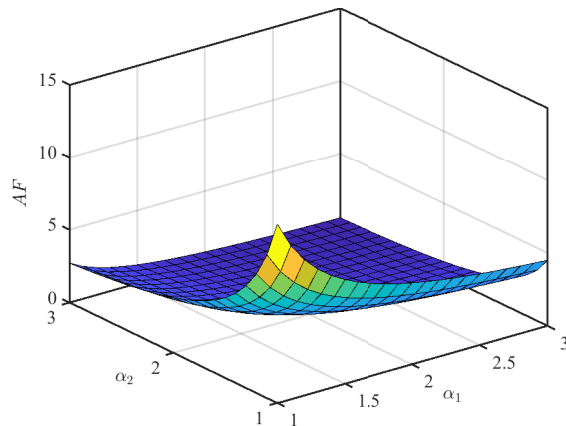


Fig. 8: AF of cascaded  $\alpha - \kappa - \mu$  shadowed channel

In Fig 7(a), we kept  $\kappa_1 = 5.0, \mu_1 = 1.2, m_1 = 3.6$  and  $\alpha_2 = 2.0, \kappa_2 = 2.1, \mu_2 = 3.0, m_2 = 1.0$  with  $\bar{\gamma}_2 = 0$  dB. Threshold SNR, *i.e.*,  $\gamma_{th}$  is set to be 5 dB. The OP of the cascade system with varying values  $\bar{\gamma}_1$  is plotted for different values of  $\alpha_1$ . Results demonstrate that the OP decreases as  $\alpha_1$  increases. This trend can also be verified through AF values shown in Fig. 8 where we can observe that the AF decreases as either  $\alpha_1$  or  $\alpha_2$  increases. Hence, the degrading effect of fading will be less for high values of  $\alpha_1$  or  $\alpha_2$ . Similarly in Fig. 7(b) we kept  $\alpha_1 = 2.0, \kappa_1 =$

5.0,  $\mu_1 = 1.2$ ,  $m_1 = 3.6$  and  $\kappa_2 = 2.1$ ,  $\mu_2 = 3.0$ ,  $m_2 = 1.0$  then we changed the value of  $\alpha_2$ . It is observed that as  $\alpha$  increases, the OP decreases. However, the effect is not independent of other parameters as in Fig. 7(a) the impact of increasing  $\alpha$  is more dominant compared to Fig. 7(b) where it saturates for  $\alpha_2 = 2.5$ . One reason for this behavior may be that the  $\kappa_1 > \kappa_2$  dominates the overall link. These theoretical results can be further used in resource allocation optimization problems where the objective is to minimize the OP.

### B. Results for Physical Layer Security

This subsection presents the results for physical layer security metrics such as SOP and SPSC for  $\alpha - \kappa - \mu$  shadowed fading. In Fig. 9 and 11, the fading parameters of legitimate (source to destination) link are  $\kappa_{SD} = 5.0$ ,  $\mu_{SD} = 2.1$ ,  $m_{SD} = 10.0$ ,  $\bar{\gamma}_{SD} = 0$  dB. Also, the fading parameters of the source to eavesdropper links are  $\kappa_{SE} = 4.2$ ,  $\mu_{SE} = 1.5$ ,  $m_{SE} = 4.0$ . The target secrecy rate is  $R_s = 1$ . In Fig. 9(a), we have plotted the SOP versus  $\bar{\gamma}_{SE}$  for  $\alpha_{SE} = 2.0$  and different values of  $\alpha_{SD}$ . Here, one interesting point to note is that a higher value of  $\alpha_{SD}$  is not better for all the values of  $\bar{\gamma}_{SE}$  as one can observe from the figure that a lower  $\alpha_{SD}$  is having lower SOP for  $\bar{\gamma}_{SE} > 0$  dB. Similarly, in Fig. 9(b), we have plotted the SOP versus  $\bar{\gamma}_{SE}$  for  $\alpha_{SD} = 2.0$  and different values of  $\alpha_{SE}$ . Here, also we can see a crossover in the behavior of SOP at  $\bar{\gamma}_{SE} = -5$  dB. Intuitively, an increase in  $\alpha_{SE}$  should be detrimental to SOP but the result reveals that it is not independent from the value of  $\bar{\gamma}_{SE}$ . Increasing  $\alpha_{SE}$  has detrimental effect only when the  $\bar{\gamma}_{SE} \geq 0$  dB.

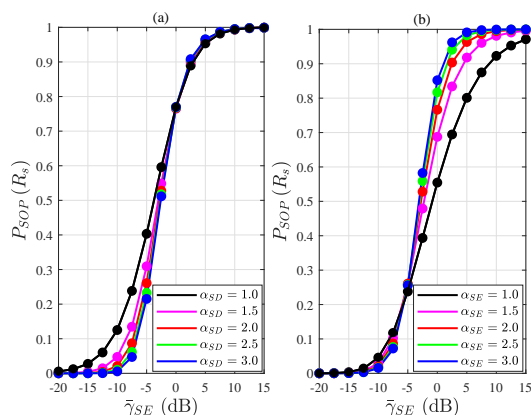


Fig. 9: SOP for  $\alpha - \kappa - \mu$  shadowed fading for varying  $\bar{\gamma}_{SE}$

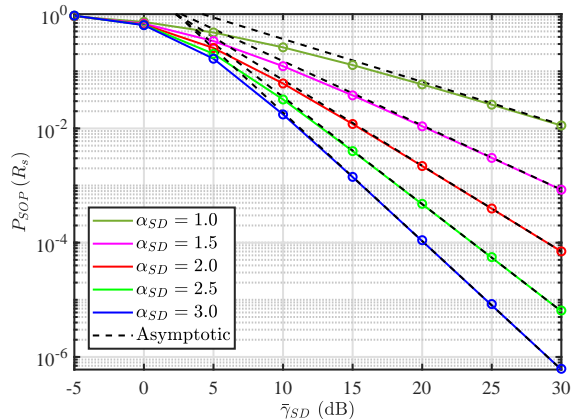


Fig. 10: SOP for  $\alpha - \kappa - \mu$  shadowed fading for varying  $\bar{\gamma}_{SD}$

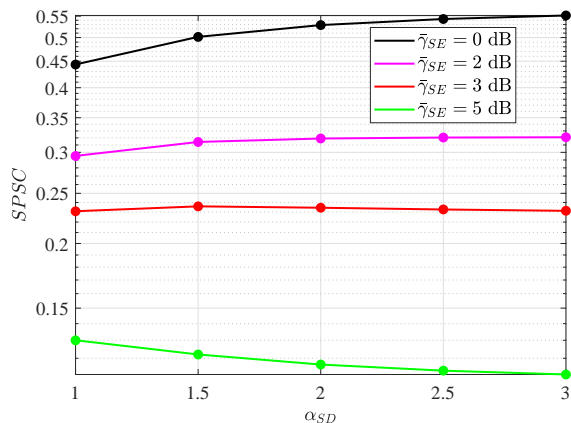


Fig. 11: SPSC for  $\alpha - \kappa - \mu$  shadowed fading

Fig. 11 present the SPSC versus  $\alpha_{SD}$  for  $\alpha_{SE} = 2.0$  and different values of  $\bar{\gamma}_{SE}$ . It is interesting to note that SPSC does not have a monotonic relation with  $\alpha_{SD}$ , *i.e.*, we can't always expect a better SPSC for higher  $\alpha_{SD}$ . We can observe from the figure that for the high value of  $\bar{\gamma}_{SE}$  SPSC saturates or even decreases with increasing  $\alpha_{SD}$ .

### C. Results for IRS-Assisted Communication System

In this subsection, we have presented the results of the IRS-assisted communication system. We consider a simulation setup such that the **S**, **IRS**, and **D** are placed at  $(0, 0)$ ,  $(0, 10)$ , and  $(90, 0)$ , respectively. The path-loss coefficient  $\beta$  is chosen to be 4 and  $\gamma_s = 73$  dB. Other fading parameters are as follows  $\kappa_{SD} = 0.8$ ,  $\mu_{SD} = 1.5$ ,  $m_{SD} = 4.0$ ,  $\kappa_{SR} = 2.1$ ,  $\mu_{SR} = 3.0$ ,  $m_{SR} = 4.4$ , and  $\kappa_{RD} = 5.0$ ,  $\mu_{RD} = 1.2$ ,  $m_{RD} = 2.8$ . The simulation parameter are similar to [23]. We set

$\alpha_{SD} = 2.0$ ,  $\alpha_{SR} = 3.0$ , and  $\alpha_{RD} = 1.0$  unless mentioned otherwise. In Fig. 12, we plotted the OP for different values of  $N$ . It is evident from Fig. 12 that the approximation derived in Section VIII-C matches with simulated values. Also, as the number of IRS elements increases, the OP decreases. Next, in Fig. 13, we plotted the OP for different  $\alpha_{SD}$ . Interestingly, the higher value of  $\alpha_{SD}$  has a positive impact only up to a certain threshold. After that, we observed the opposite behavior. We can see in the figure that for  $\gamma_{th} < 0$  dB, OP is less for higher  $\alpha_{SD}$  value, but for  $\gamma_{th} > 0$  dB; OP is higher for higher  $\alpha_{SD}$  values.

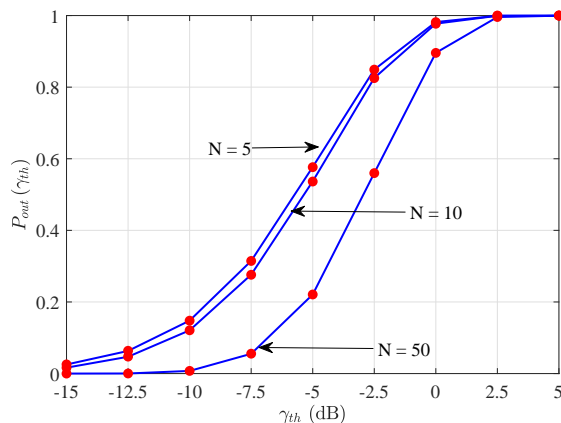


Fig. 12: OP of IRS-Assisted Communication System for various  $N$

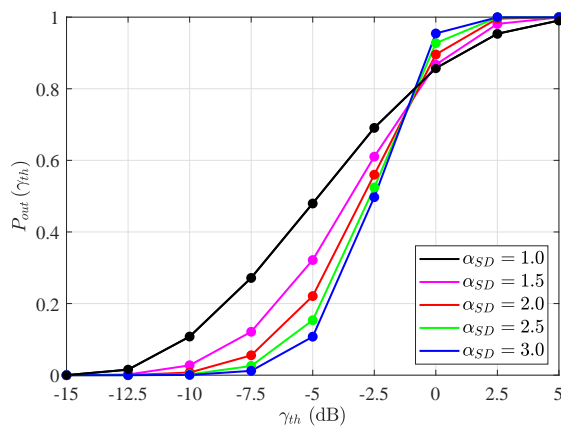


Fig. 13: OP of IRS-Assisted Communication System for various  $\alpha_{SD}$

Fig. 14 and 15 presents the OP for different values of  $\alpha_{SR}$  and  $\alpha_{RD}$ , respectively. We can observe that the OP decreases as  $\alpha_{SR}$  or  $\alpha_{RD}$  increases. This is justified as we have seen in Fig.

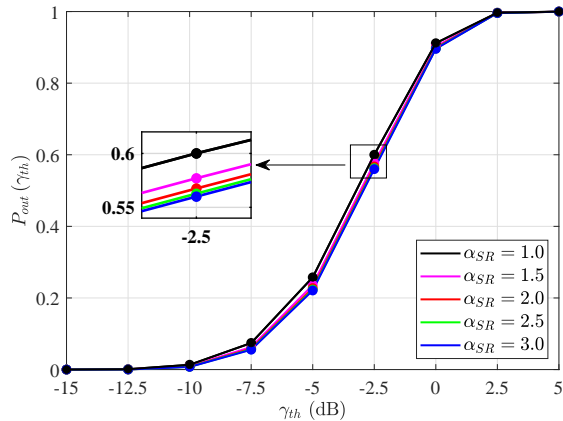


Fig. 14: OP of IRS-Assisted Communication System for various  $\alpha_{SR}$

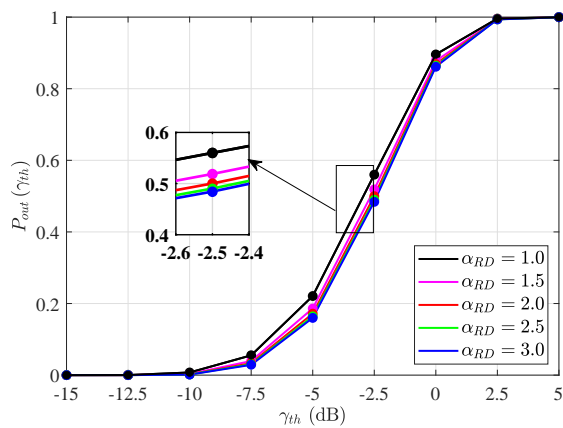


Fig. 15: OP of IRS-Assisted Communication System for various  $\alpha_{RD}$

8 that the amount of fading decreases for a cascade channel as the  $\alpha$  parameter increases for either of the links.

## X. CONCLUSION

This paper presents the series expression for PDF, CDF, and MGF of the product and ratio of two  $\alpha - \kappa - \mu$  shadowed RV. The series expression is obtained via a direct application of Mellin transformation. We have also derived a Laplace-type integral representation for the product and ratio statistics PDF. Some typical examples of wireless communication applications, like cascaded systems and physical layer security, are provided. While we have provided a 6G application, namely an IRS-assisted communication system, the fading model considered in this paper is quite general and encompasses typically used fading models. Hence, we hope our results can be

used for other emerging applications. These theoretical results are important not only to assess the performance of the considered application but also helpful in proper resource allocation. An interesting extension for this work is considering the product of an arbitrary number of  $\alpha - \kappa - \mu$  shadowed RVs.

## REFERENCES

- [1] M.-S. Alouini and M. K. Simon, "Dual diversity over correlated log-normal fading channels," *IEEE Transactions on Communications*, vol. 50, no. 12, pp. 1946–1959, 2002.
- [2] A. Abdi and M. Kaveh, "On the utility of gamma pdf in modeling shadow fading (slow fading)," in *1999 IEEE 49th Vehicular Technology Conference (Cat. No. 99CH36363)*, vol. 3. IEEE, 1999, pp. 2308–2312.
- [3] M. D. Yacoub, "The  $\kappa$ - $\mu$  distribution and the  $\eta$ - $\mu$  distribution," *IEEE Antennas and Propagation Magazine*, vol. 49, no. 1, pp. 68–81, 2007.
- [4] J. F. Paris, "Statistical characterization of  $\kappa - \mu$  shadowed fading," *IEEE Transactions on Vehicular Technology*, vol. 63, no. 2, pp. 518–526, 2013.
- [5] M. D. Yacoub, "The  $\alpha - \mu$  distribution: A physical fading model for the stacy distribution," *IEEE Transactions on Vehicular Technology*, vol. 56, no. 1, pp. 27–34, 2007.
- [6] P. Ramirez-Espinosa, J. M. Moualeu, D. B. da Costa, and F. J. Lopez-Martinez, "The  $\alpha - \kappa - \mu$  shadowed fading distribution: statistical characterization and applications," in *2019 IEEE Global Communications Conference (GLOBECOM)*. IEEE, 2019, pp. 1–6.
- [7] S. K. Yoo, S. L. Cotton, P. C. Sofotasios, M. Matthaiou, M. Valkama, and G. K. Karagiannidis, "The fisher - snedecor  $\mathcal{F}$  distribution: A simple and accurate composite fading model," *IEEE Communications Letters*, vol. 21, no. 7, pp. 1661–1664, 2017.
- [8] H. Du, J. Zhang, K. P. Peppas, H. Zhao, B. Ai, and X. Zhang, "On the distribution of the ratio of products of fisher-snedecor  $\mathcal{F}$  random variables and its applications," *IEEE Transactions on Vehicular Technology*, vol. 69, no. 2, pp. 1855–1866, 2019.
- [9] B. Talha and M. Paetzold, "Channel models for mobile-to-mobile cooperative communication systems: A state of the art review," *IEEE Vehicular Technology Magazine*, vol. 6, no. 2, pp. 33–43, 2011.
- [10] M. Di Renzo, A. Zappone, M. Debbah, M. S. Alouini, C. Yuen, J. de Rosny, and S. Tretyakov, "Smart radio environments empowered by reconfigurable intelligent surfaces: How it works, state of research, and the road ahead," *IEEE Journal on Selected Areas in Communications*, vol. 38, no. 11, pp. 2450–2525, 2020.
- [11] Q. Wu and R. Zhang, "Towards smart and reconfigurable environment: Intelligent reflecting surface aided wireless network," *IEEE Communications Magazine*, vol. 58, no. 1, pp. 106–112, 2019.
- [12] Zhang, Jiayi and Björnson, Emil and Matthaiou, Michail and Ng, Derrick Wing Kwan and Yang, Hong and Love, David J., "Prospective multiple antenna technologies for beyond 5G," *IEEE Journal on Selected Areas in Communications*, vol. 38, no. 8, pp. 1637–1660, 2020.
- [13] K. P. Peppas, N. C. Sagias, and A. Maras, "Physical layer security for multiple-antenna systems: A unified approach," *IEEE Transactions on Communications*, vol. 64, no. 1, pp. 314–328, 2015.
- [14] B. D. Carter and M. D. Springer, "The distribution of products, quotients and powers of independent h-function variates," *SIAM Journal on Applied Mathematics*, vol. 33, no. 4, pp. 542–558, 1977.
- [15] N. Fasarakis-Hilliard, P. N. Alevizos, and A. Bletsas, "Coherent detection and channel coding for bistatic scatter radio sensor networking," *IEEE Transactions on Communications*, vol. 63, no. 5, pp. 1798–1810, 2015.

- [16] P. N. Alevizos, A. Bletsas, and G. N. Karystinos, "Noncoherent short packet detection and decoding for scatter radio sensor networking," *IEEE Transactions on Communications*, vol. 65, no. 5, pp. 2128–2140, 2017.
- [17] H. Lu, Y. Chen, and N. Cao, "Accurate approximation to the pdf of the product of independent rayleigh random variables," *IEEE Antennas and Wireless Propagation Letters*, vol. 10, pp. 1019–1022, 2011.
- [18] P. N. Alevizos, K. Tountas, and A. Bletsas, "Multistatic scatter radio sensor networks for extended coverage," *IEEE Transactions on Wireless Communications*, vol. 17, no. 7, pp. 4522–4535, 2018.
- [19] J. Salo, H. M. El-Sallabi, and P. Vainikainen, "The distribution of the product of independent Rayleigh random variables," *IEEE Transactions on Antennas and Propagation*, vol. 54, no. 2, pp. 639–643, 2006.
- [20] G. K. Karagiannidis, N. C. Sagias, and P. T. Mathiopoulos, " $N^*$  Nakagami: a novel stochastic model for cascaded fading channels," *IEEE Transactions on Communications*, vol. 55, no. 8, pp. 1453–1458, 2007.
- [21] F. Yilmaz and M.-S. Alouini, "Product of the powers of generalized Nakagami- $m$  variates and performance of cascaded fading channels," in *GLOBECOM 2009-2009 IEEE Global Telecommunications Conference*. IEEE, 2009, pp. 1–8.
- [22] D. Selimis, K. P. Peppas, G. C. Alexandropoulos, and F. I. Lazarakis, "On the performance analysis of ris-empowered communications over Nakagami- $m$  fading," *IEEE Communications Letters*, vol. 25, no. 7, pp. 2191–2195, 2021.
- [23] M. Charishma, A. Subhash, S. Shekhar, and S. Kalyani, "Outage probability expressions for an IRS-assisted system with and without source-destination link for the case of quantized phase shifts in  $\kappa - \mu$  fading," *IEEE Transactions on Communications*, pp. 1–1, 2021.
- [24] N. Bhargav, C. R. N. da Silva, Y. J. Chun, E. J. Leonardo, S. L. Cotton, and M. D. Yacoub, "On the product of two  $\kappa$ - $\mu$  random variables and its application to double and composite fading channels," *IEEE Transactions on Wireless Communications*, vol. 17, no. 4, pp. 2457–2470, 2018.
- [25] C. R. N. da Silva, E. J. Leonardo, and M. D. Yacoub, "Product of two envelopes taken from  $\alpha - \mu$ ,  $\kappa - \mu$ , and  $\eta - \mu$  distributions," *IEEE Transactions on Communications*, vol. 66, no. 3, pp. 1284–1295, 2018.
- [26] M. Bilim, "Cascaded double fading channels: A case of  $\kappa - \mu$  shadowing," *Physical Communication*, p. 101649, 2022.
- [27] A. Abdi, W. C. Lau, M.-S. Alouini, and M. Kaveh, "A new simple model for land mobile satellite channels: First- and second-order statistics," *IEEE Transactions on Wireless Communications*, vol. 2, no. 3, pp. 519–528, 2003.
- [28] N. A. Sarker, A. Badrudduza, S. R. Islam, S. H. Islam, M. K. Kundu, I. S. Ansari, and K.-S. Kwak, "On the intercept probability and secure outage analysis of mixed ( $\alpha$ - $\kappa$ - $\mu$ )-shadowed and Málaga turbulent models," *IEEE Access*, vol. 9, pp. 133 849–133 860, 2021.
- [29] A. Badrudduza, S. H. Islam, M. K. Kundu, and I. S. Ansari, "Secrecy performance of  $\alpha$ - $\kappa$ - $\mu$  shadowed fading channel," *ICT Express*, 2021.
- [30] P. Bhardwaj and S. M. Zafaruddin, "Fixed-gain af relaying for rf-thz wireless system over  $\alpha$ - $\kappa$ - $\mu$  shadowed and  $\alpha$ - $\mu$  channels," *IEEE Communications Letters*, vol. 26, no. 5, pp. 999–1003, 2021.
- [31] T. Wu, J. Zeng, N. Ye, W. Feng, and T. Lv, "Accurate asymptotic characterization of  $\alpha$ - $\kappa$ - $\mu$  shadowed fading channel with application to secure urllc," *IEEE Communications Letters*, vol. 27, no. 4, pp. 1100–1104, 2023.
- [32] S. Belmoubarik, G. Aniba, and B. Elgraini, "Secrecy capacity of a Nakagami- $m$  fading channel in the presence of cooperative eavesdroppers," in *Proceedings of 2014 Mediterranean Microwave Symposium (MMS2014)*. IEEE, 2014, pp. 1–6.
- [33] S. Iwata, T. Ohtsuki, and P.-Y. Kam, "Secure outage probability over  $\kappa - \mu$  fading channels," in *2017 IEEE international conference on communications (ICC)*. IEEE, 2017, pp. 1–6.
- [34] N. Bhargav, S. L. Cotton, and D. E. Simmons, "Secrecy capacity analysis over  $\kappa - \mu$  fading channels: Theory and applications," *IEEE Transactions on Communications*, vol. 64, no. 7, pp. 3011–3024, 2016.

- [35] M. Srinivasan and S. Kalyani, "Secrecy capacity of  $\kappa - \mu$  shadowed fading channels," *IEEE Communications Letters*, vol. 22, no. 8, pp. 1728–1731, 2018.
- [36] Q. Tao, J. Wang, and C. Zhong, "Performance analysis of intelligent reflecting surface aided communication systems," *IEEE Communications Letters*, 2020.
- [37] D. Kudathanthirige, D. Gunasinghe, and G. Amarasuriya, "Performance analysis of intelligent reflective surfaces for wireless communication," in *ICC 2020-2020 IEEE International Conference on Communications (ICC)*. IEEE, 2020, pp. 1–6.
- [38] S. Atapattu, R. Fan, P. Dharmawansa, G. Wang, J. Evans, and T. A. Tsiftsis, "Reconfigurable intelligent surface assisted two-way communications: Performance analysis and optimization," *IEEE Transactions on Communications*, vol. 68, no. 10, pp. 6552–6567, 2020.
- [39] H. M. Srivastava and P. W. Karlsson, *Multiple Gaussian hypergeometric series*. Ellis Horwood, 1985.
- [40] M. D. Springer, *The algebra of random variables*. New York: Wiley, 1979.
- [41] A. M. Mathai, R. K. Saxena, and H. J. Haubold, *The H-function: theory and applications*. Springer Science & Business Media, 2009.
- [42] A. A. Kilbas, L. Rodríguez-Germá, M. Saigo, R. Saxena, and J. J. Trujillo, "The krätzel function and evaluation of integrals," *Computers & Mathematics with Applications*, vol. 59, no. 5, pp. 1790–1800, 2010.
- [43] I. S. Gradshteyn and I. M. Ryzhik, *Table of integrals, series, and products*. Academic Press, 2007.
- [44] G. M. Cordeiro and A. J. Lemonte, "The mcdonald inverted beta distribution," *Journal of the Franklin Institute*, vol. 349, no. 3, pp. 1174–1197, 2012.
- [45] A. M. Mathai and H. J. Haubold, *Special functions for applied scientists*. Springer, 2008, vol. 4.
- [46] M. Abramowitz and I. A. Stegun, *Handbook of mathematical Functions*. Dover Publications, 1965.
- [47] M. K. Simon and M.-S. Alouini, *Digital communication over fading channels*. John Wiley & Sons, 2005, vol. 95.
- [48] M. Bloch, J. Barros, M. R. Rodrigues, and S. W. McLaughlin, "Wireless information-theoretic security," *IEEE Transactions on Information Theory*, vol. 54, no. 6, pp. 2515–2534, 2008.
- [49] L. Fan, X. Lei, T. Q. Duong, M. ElKashlan, and G. K. Karagiannidis, "Secure multiuser communications in multiple amplify-and-forward relay networks," *IEEE Transactions on Communications*, vol. 62, no. 9, pp. 3299–3310, 2014.
- [50] E. Björnson, Ö. Özdogan, and E. G. Larsson, "Intelligent reflecting surface versus decode-and-forward: How large surfaces are needed to beat relaying?" *IEEE Wireless Communications Letters*, vol. 9, no. 2, pp. 244–248, 2019.
- [51] D. Li, "Ergodic Capacity of Intelligent Reflecting Surface-Assisted Communication Systems with Phase Errors," *IEEE Communications Letters*, 2020.
- [52] F. A. De Figueiredo, M. S. Facina, R. C. Ferreira, Y. Ai, R. Ruby, Q.-V. Pham, and G. Fraidenraich, "Large intelligent surfaces with discrete set of phase-shifts communicating through double-Rayleigh fading channels," *IEEE Access*, vol. 9, pp. 20 768–20 787, 2021.
- [53] G. Casella and R. L. Berger, *Statistical inference*. Cengage Learning, 2021.
- [54] E. Martos-Naya, J. Romero-Jerez, and J. Paris, "A MATLAB™ program for the computation of the confluent hypergeometric function  $\phi_2$ ," 2016.